Bull. Mater. Sci., Vol. 35, No. 4, August 2012, pp. 505–511. © Indian Academy of Sciences.

Influence of nitrogen flow rates on materials properties of CrN_x films grown by reactive magnetron sputtering

B SUBRAMANIAN*, **K PRABAKARAN** and **M JAYACHANDRAN**

Electrochemical Materials Science Division, CSIR- Central Electrochemical Research Institute, Karaikudi 630 006, India

MS received 9 April 2011; revised 17 October 2011

Abstract. **Chromium nitride (CrN) hard thin films were deposited on different substrates by reactive direct current (d.c.) magnetron sputtering with different nitrogen flow rates. The X-ray diffraction patterns showed mixed Cr_2N and CrN phases. The variations in structural parameters are discussed. The grain size increased with increasing nitrogen flow rates. Scanning electron microscopy image showed columnar and dense microstructure with varying nitrogen flow rates. An elemental analysis of the samples was realized by means of energy dispersive spectroscopy. The electrical studies indicated the semiconducting behaviour of the films at the nitrogen flow rate of 15 sccm.**

Keywords. **Thin films; magnetron sputtering; chromium nitride; X-ray diffraction.**

1. Introduction

Surface modification by means of thin film deposition is an important industrial process which is used to protect base materials against wear, fatigue, corrosion and many other surface related damage phenomena (Olaya *et al* 2007). Transition metal nitrides having bonds of a mixed nature of covalent, ionic and metallic character are of technological importance due to the combination of their functional properties that are associated with their unusual electronic bonding such as high hardness, high melting point and oxidation resistance (Olaya *et al* 2005). These coatings have found widespread use as hard wear protective coatings for cutting tools and wear applications, as diffusion barriers in micro electronic applications, and as corrosion and abrasion-wear resistant layers on optical and mechanical components (Deniel *et al* 2009). TiN and CrN are the most extensively investigated hard coatings. It is known that TiN coatings are not always corrosion resistant due to the micro defect in the coatings. CrN coatings exhibit relatively dense microstructure and provide high wear and corrosion resistance (Grips *et al* 2006). In PVD coatings, intrinsic stress is generated by reactions, phase formations, energetic particle bombardment, etc. The change in temperature differential in the expansion or contraction of dissimilar layered materials results in a variation of the residual stress along the thickness direction. The stress translates between the coating and the substrate interface, causing the coated system to contract, elongate or bend. Buckling may occur only at a critical value of compressive stress. The stress depends on thickness of the materials. A great advantage of CrN is that the internal stresses are very low, due to which coatings with thickness of more than 40 μm can be obtained on a variety of engineering substrates. On the other hand, TiN coatings can be deposited only with a thickness of less than 10 μm on account of high internal stresses and consequent poor adhesion. The friction coefficient is also very low for CrN thin films (Barshilia *et al* 2006). The main advantage associated with the deposition of CrN thin film is low deposition temperature, and this makes it suitable for deposition onto temperature-sensitive materials and low melting point metals (Yoo *et al* 2007). In addition, its characteristic silver colour has extended its application towards the decorative sector. In fact, sectors such as the automotive or the ceramic industry are considering CrN as a feasible alternative to galvanic hard chromium (Fuentes *et al* 2005). There are two types of crystal structure for chromium nitride, i.e. CrN and Cr_2N, with their components ratio controlled by apparatus geometry and deposition techniques (Novinrooz and Seyedi 2006). The Cr_2N phase exhibits a higher hardness. On the other hand, the CrN phase is also interesting due to its magnetic, optical and electronic properties (Novakovic *et al* 2007). The compositions, phase structure, texture, grain size and properties of CrN coating are strongly influenced by the reactive nitrogen gas content, the applied substrate bias and substrate temperature. Depending on nitrogen content, the d.c. magnetron sputtered CrN coatings may consist of Cr, β-Cr_2N, c-CrN and/or mixture of these phases (Lin *et al* 2009). The CrN thin films were deposited by various methods such as ion source middle frequency magnetron sputtering, unbalanced magnetron sputtering (Zou *et al* 2009), rf reactive sputtering (Inoue *et al* 2009), pulsed d.c. magnetron sputtering (Li *et al* 2009), metal vapour vacuum arc (Chen *et al* 2004), arc discharge (Shen *et al* 2008), e-beam PVD (Conde *et al* 2006), hollow cathode discharge gun (Novinrooz and Seyedi 2006). The

*Author for correspondence (bsmanian@cecri.res.in)

protection capability of these nitrides strongly depends on the deposition condition.

In this study, influence of nitrogen flow rates on the materials properties of reactive magnetron sputtered chromium nitride (CrN_x) thin films were investigated and also the emphasis is placed on mixed phase formation.

2. Experimental

CrN thin films of 1·5 μm thickness with different nitrogen flow rates were deposited on well-cleaned glass substrates and Si (100) wafers using a d.c. magnetron sputter deposition unit HIND HIVAC. High purity argon (99·99%) was fed into the vacuum chamber for plasma generation. The substrates were etched for 5 min at a d.c. power of 50 W and an argon pressure of 10 m Torr (1·33 Pa). The optimized deposition parameters for CrN sputtering are summarized in table 1.

Table 1. Deposition parameters for CrN reactive sputtering.

Objects	Specification
Target (2″Dia)	Cr (99·9%)
Substrate	Glass and Si (100)
Target to substrate distance	50 mm
Ultimate vacuum	1×10^{-6} m bar
Operating vacuum	2×10^{-3} m bar
Sputtering gas	Ar: 49 sccm
	N_2: 0–20 sccm
Power	50 Watt
Substrate temperature	200 °C

X-ray analysis was conducted in PANalytical-X'Pert Pro using CuK_α (1·514 Å) and a thin film attachment with a parallel plate collimator, 0·18° and the incidence angle being 1°. The electrical studies were carried out by four-probe set up model DFP-20. The surface morphology of the coatings was studied by scanning electron microscopy (SEM) using a Hitachi S 3000H microscope equipped with thermoelectron corporation energy dispersive X-ray (EDX) spectrometer. The surface topography of the films was studied using NanoNavi SPI3800N atomic force microscopy (AFM).

3. Results and discussion

XRD results as shown in figure 1 indicate that the crystallography structure of sputter-deposited CrN thin films depends on the nitrogen content in the sputtering process. By reactive magnetron sputtering, different phases of CrN_x like Cr, Cr+N, Cr+N+Cr_2N, Cr_2N+CrN, CrN can be obtained by varying the nitrogen content. The structures of the CrN_x coatings are strongly determined by different processes,

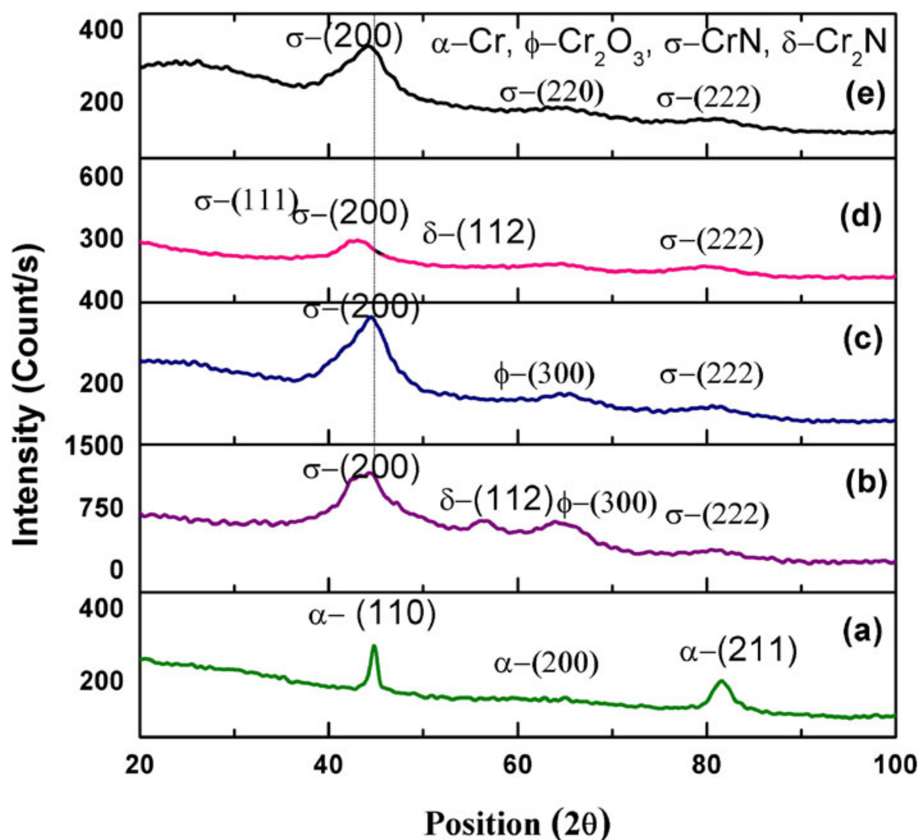

Figure 1. XRD patterns as functions of nitrogen flow rates: (a) 0 sccm, (b) 5 sccm, (c) 10 sccm, (d) 15 sccm and (e) 20 sccm.

which take place both cathode and sample surface during the sputtering process. All these processes are determined by the discharge parameters, viz. voltage and intensity, relative Ar/N_2 ratio, pressure, pumping rate, etc. The interplay between the different plasma parameters in medium frequency magnetron sputtering system controlling the CrN_x phases could be the reason for amorphous phase formation reported in the literature (Inoue *et al* 2002).

XRD pattern (figure 1) confirms that the deposited films are polycrystalline in nature. For the film deposited at 0 sccm, the pattern shows Cr (110), (200) and (211) orientations. Mixed phases were observed at a low nitrogen flow rate of 5 sccm. The film contains face centred cubic CrN phase with preferred orientations along (200) and (222), orientation along (112) of hexagonal Cr_2N phase and orientation along (300) of Cr_2O_3. This result is in good agreement with Cunha *et al* (1999) who found that CrN exhibited a (200) texture.

At the nitrogen flow rate of 10 sccm, the film contains mainly CrN phase with a orientation of (200) and with low intensity along (222) and Cr_2O_3 phase along (300) with low intensity. At the nitrogen flow rate of 15 sccm, the pattern shows CrN phase with preferred orientation (200) and weak peak along (111), (222) and Cr_2N phase along (112) orientations. When nitrogen flow is increased to 20 sccm, only CrN phase is observed with the preferred orientation (200) and along (220) and (222) with weaker intensity. The formation of Cr_2N phase occurs only in narrow region of nitrogen flow rate as reported in the literature (Wei *et al* 2001). At higher nitrogen flow rate, the intensity of (200) orientation was found to decrease which might be due to the less content of Cr ions sputtering from the target at higher nitrogen flow rate and cause changes in the growth orientation of CrN phase. No purely single-phase CrN films were obtained even when the flow rate was increased to 20 sccm. This is due to the unbalanced growing conditions of magnetron sputtering, which were due to the rapid solidification of highly energetic particles (Zhang *et al* 2007). Pelleg *et al* (1991) have shown that for these types of material, the actual plane of lowest surface energy is (2 0 0). They also suggested that the (1 1 1) plane in metal nitride possesses lowest strain energy, due to anisotropy of Young's modulus, and that this frequently observed orientation is due to a minimization of strain energy. Its alignment normal to the growing direction will minimize the total energy under strain-energy dominated growth (Albano *et al* 2006). Other factors that may affect the preferred orientation and grain size of these coatings include deposition rate and coating thickness. It is due to the fact that lower sputtering rates enhance the energetic discharge species to deposit atoms on the growing coatings and account for the (2 0 0) preferred orientation as well as increase in grain growth (Huang and Yeh 2009).

The structural parameters derived from XRD pattern are given in table 2. Increasing nitrogen flow rate causes all diffraction peak shifts to lower angles, indicating the expansion of lattice constant by excess N atoms. The values of lattice parameter shown in table 2 are in close agreement with the lattice parameter of bulk CrN (4·140 Å). Zhao *et al* (2004) reported that the lattice parameter of the CrN_{1-x} increases sharply with increasing nitrogen flow. The cubic CrN_{1-x} phase from low nitrogen deposition possesses more 'vacancies' in N-lattice sites, relative to the stoichiometric CrN. Such a more 'open' structure tends to be more receptive to N atoms, which explains why the lattice parameter increases more rapidly near the lower side of the nitrogen flow. At high nitrogen flows, however, the cubic CrN_{1-x} phase approach to the stoichiometric CrN and the incorporation of N atoms becomes more difficult. As a result, the lattice parameter increases only slightly and reaches nearly the value reported in ICSD for the stoichiometric CrN.

The average grain sizes were calculated for CrN (200) peak from XRD pattern by using Scherrer's formula. When the nitrogen flow rate increases from 5 sccm to 20 sccm, the grain size is found to increase linearly. This is due to the degree and types of nucleation which are determined by the energy of the particle sputtered from the target (Gao *et al* 2007). The increase in grain size can be attributed to the fact that at higher N_2 flow rate the expansion of plasma is less and hence mobility of reactants decreases and simultaneously particle density increases (Shukla and Khare 2008).

The mean free paths of gas particles are shorter and they decrease with the increase in nitrogen flow rate. The decrease of mean free path also means less energy and momentum delivery on the substrate by ion impingement. This leads to lesser extent of surface damage and fewer nucleation sites, which may result in larger grain size. Initially the tensile stress increases from 2·8 GPa to 7·3 GPa with increase of nitrogen flow rate to 10 sccm. The increasing tensile stress is due to the formation of near stoichiometric CrN. A similar trend is observed by Inoue *et al* (2002). At this flow rate regime, increasing nitrogen flow rate introduces more

Table 2. Summary of structural parameter derived from XRD results.

N2 flow rate (sccm) (GPa)	Lattice parameter (Å)	Grain size (nm)	Dislocation density ($\times 10^{15}$ line m^{-1})	No. of crystallites ($\times 10^{18}$ m^{-2})	Strain ($\times 10^{-3}$ line^{-2}/m^{-4})	Stress
0	2·871	12·20	6·65	1·34	2·95	2·14
5	4·117	11·47	7·61	1·49	3·16	2·81
10	4·079	15·15	4·36	0·62	2·39	7·36
15	4·169	29·95	1·11	0·07	1·21	−3·52
20	4·143	28·86	1·20	0·08	1·26	−0·41

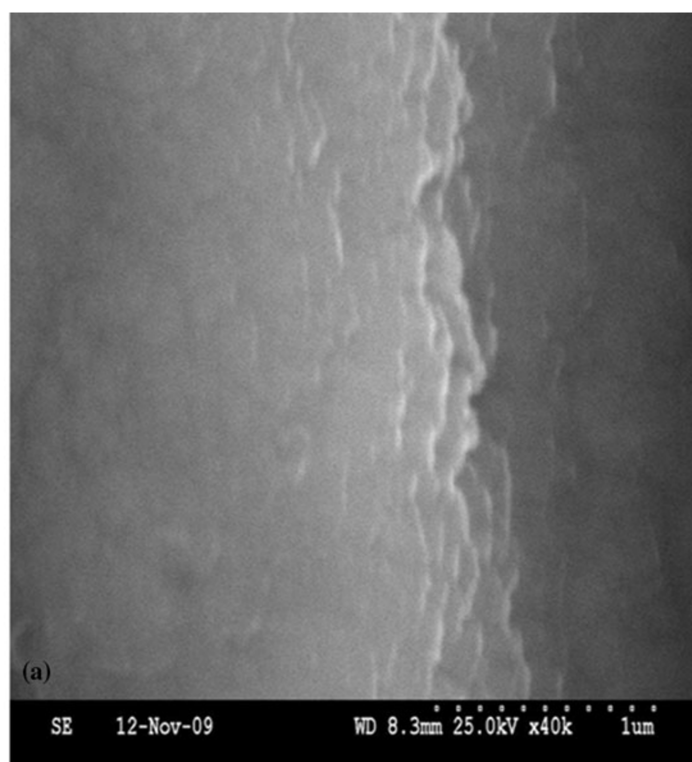

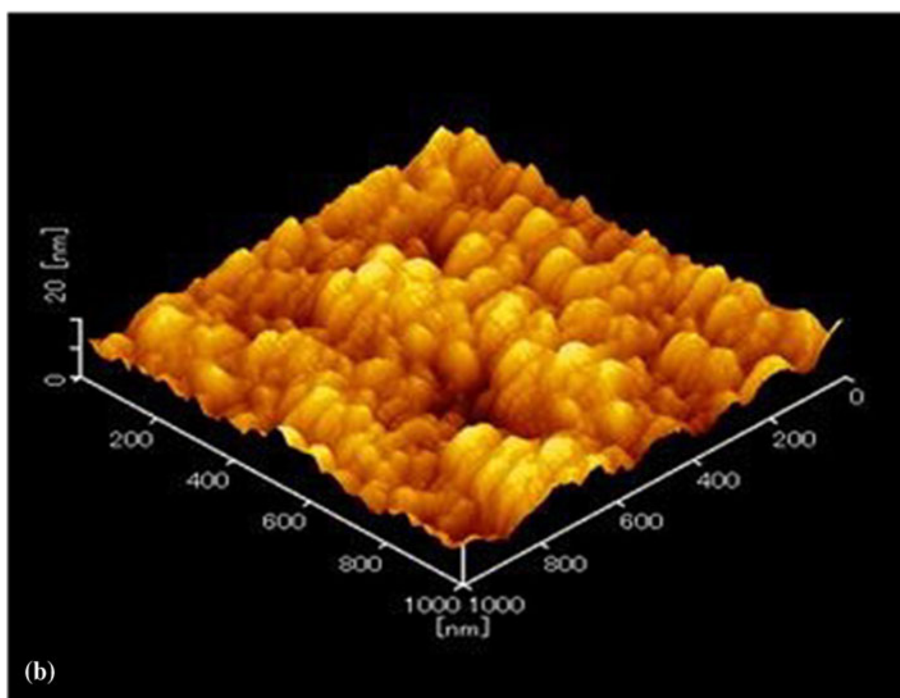

Figure 2. (**a**) Cross sectional micrograph of sputtered CrN film and (**b**) AFM image of sputtered CrN film.

nitrogen atoms into the chamber, which could react with Cr ions. On the other hand, energy of Cr ions does not substantially decrease due to the collision with gaseous particles, and therefore, Cr ions may produce atomic defects in the film when they impinge the substrate surface. The increase of defects would cause increase of the residual stress. Further on increasing the nitrogen flow rate the tensile stress decreases and becomes compressive at the N_2 rate of 15 sccm. This can be attributed to the decrease of kinetic energy of Cr ions. With increasing nitrogen flow rate, the energy of Cr ions decreases because the collision probability between Cr ions and gaseous particle increases. As a result, the capability of Cr ions to produce atomic defects decreases, and thereby decreasing the residual stress (Huang *et al* 2007).

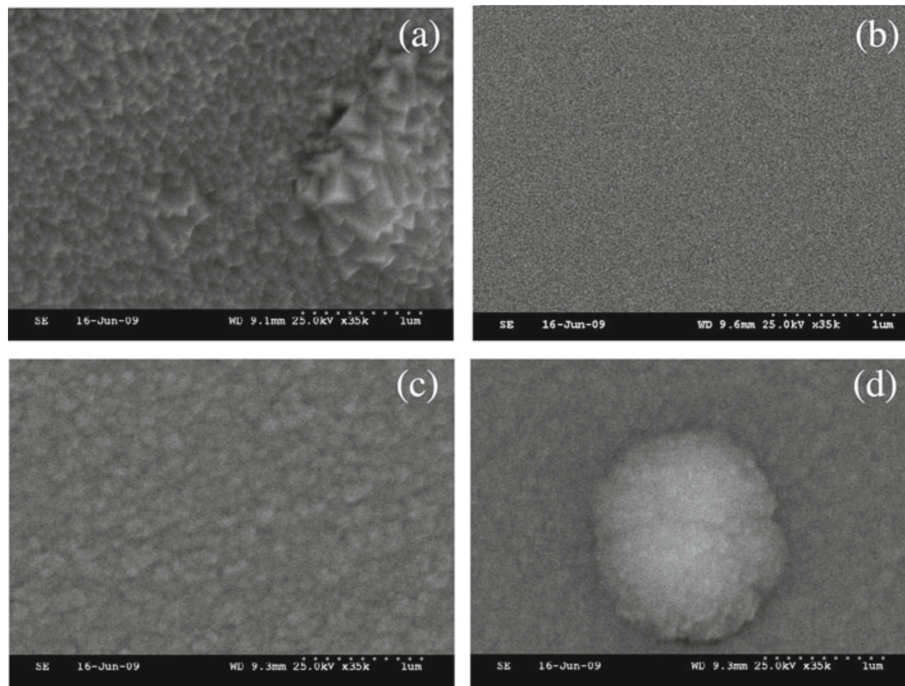

Figure 3. SEM images of CrN thin films as a function of nitrogen flow rate: (**a**) 0 sccm, (**b**) 5 sccm, (**c**) 10 sccm and (**d**) 20 sccm.

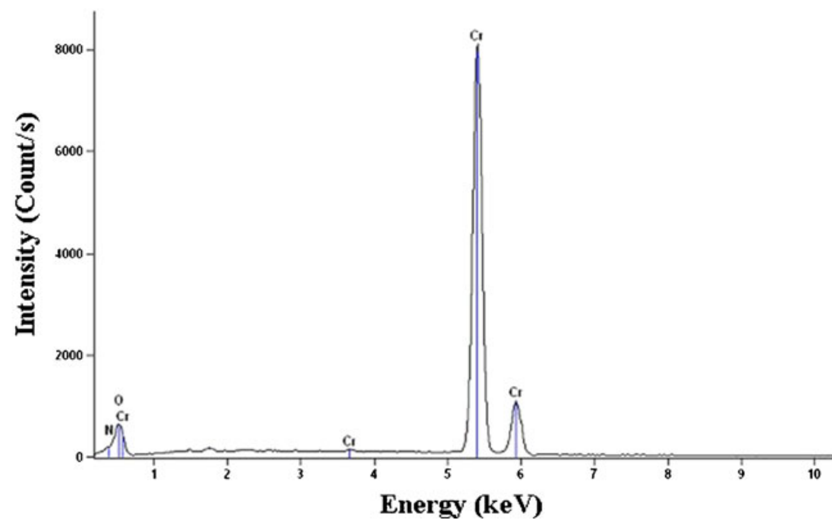

Figure 4. EDX spectrum of sputtered CrN films at nitrogen flow rate of 5 sccm.

Table 3. Composition of CrN films as determined using EDX analysis.

Element	Nitrogen flow rates (sccm)				
(Atom %)	0	5	10	15	20
O	11·23	6·75	4·37	—	—
N	—	22·05	28·42	33·65	37·08
Cr	88·77	71·20	67·21	66·35	62·92

The columnar morphology of these CrN films is shown in figures 2a and b from the cross-section analysis of SEM and AFM, respectively. Figure 3 shows the surface morphology of CrN thin films at different N_2 flow rates. At the nitrogen flow rate of 5 sccm, uniform coverage of grains over the surface of the film is observed, which may be due to the presence of mixed phases of CrN and Cr_2N as indicated by XRD pattern. Further on increasing the nitrogen flow rate to 20 sccm the films exhibit larger grain size with agglomeration in corroboration with XRD results.

To confirm the results further from the X-ray diffraction, an elemental analysis was conducted to determine the elements present in the deposited film using EDS coupled to a SEM. The compositions in at % for the CrN thin films prepared at different nitrogen flow rates are given in table 3. EDS spectrum for the film prepared at N_2 flow rate of 5 sccm where the elements are identified such as Cr and with less identity of N and O is shown in figure 3.

It can be noted that the oxygen peak is present as shown in figure 4. The reason is that chromium nitride is sensitive to oxidation in a similar way as titanium nitride (Ramos and Valmoria 2004). Another reason can also be attributed to the fact that the samples have already been exposed to the atmosphere for quite sometime before elemental analysis was conducted.There is a peak overlap between the Cr L and O K because of the energy values of Cr $L\alpha^1$ is 0·587 keV

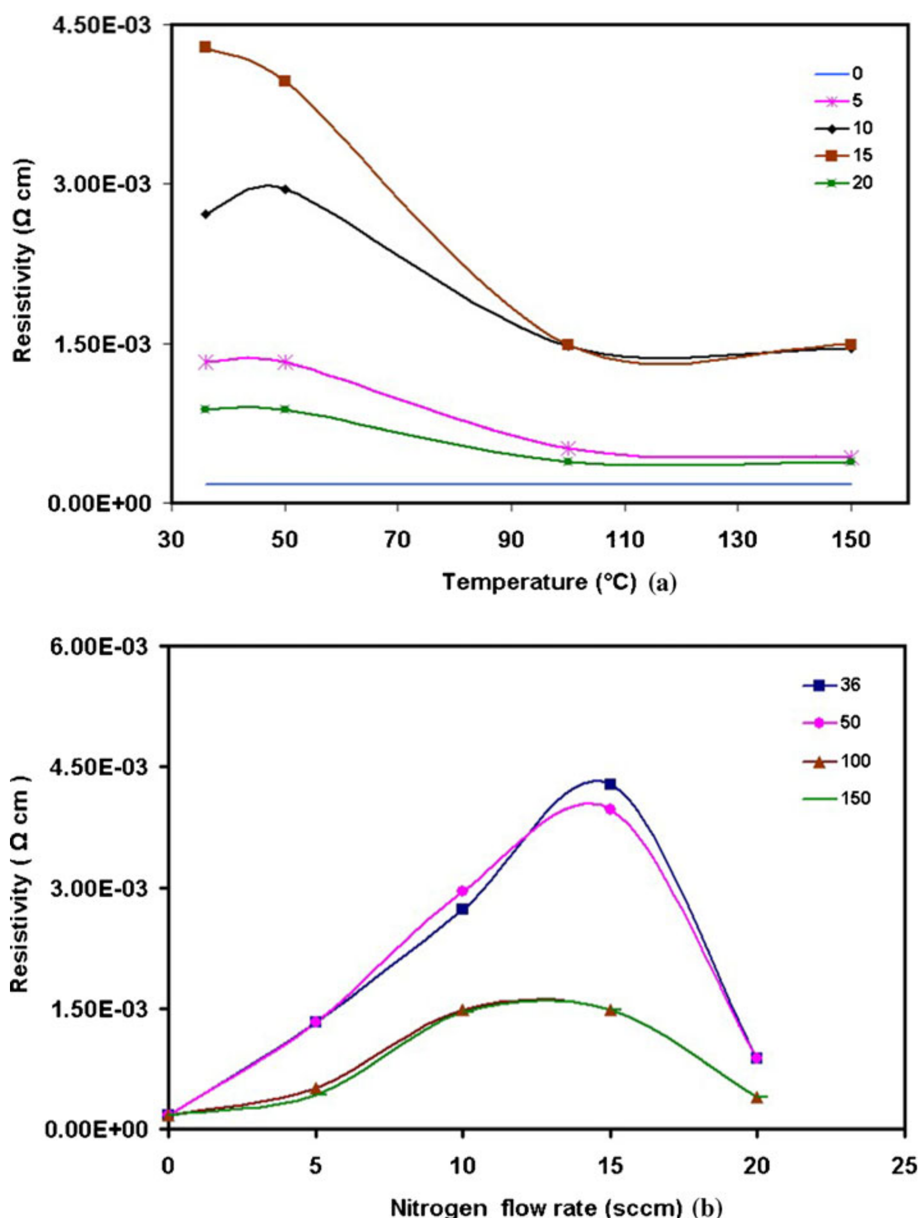

Figure 5. (**a**) Variations of resistivity as a function of temperature for different nitrogen flow rates and (**b**) variations of resistivity as a function of nitrogen flow rate for different temperatures.

and for the O K α^1 it is 0·509 keV which are closer to each other.

Figures 5a and b show variation of resistivity of the CrN thin films with temperatures in the range of 36–150 °C and at different N_2 flow rates, respectively. The resistivity of pure Cr thin film at room temperature (36°C) is about $1{\cdot}7 \times 10^{-4}$ Ω cm which is in agreement with the value of $6{\cdot}2 \times 10^{-4}$ Ω cm already reported (Zhang *et al* 2007). It varies from $1{\cdot}32 \times 10^{-3}$ to $4{\cdot}3 \times 10^{-3}$ Ω cm as N_2 flow rate is changed from 5 sccm to 15 sccm. This is in good agreement with the reported value of resistivity of $4{\cdot}52 \times 10^{-3}$ Ω cm for the CrN film grown by rf plasma assisted molecular beam epitaxy (Constatin *et al* 2004). A lower resistivity value of $8{\cdot}7 \times 10^{-4}$ Ω cm was observed at N_2 flow rate of 20 sccm at room temperature. The value initially increases with increasing temperature up to 50 °C which is due to metallic behaviour of the films. When the temperature is increased further, the resistivity exponentially decreases. This trend is due to semiconducting behaviour of CrN film beyond 50 °C as obtained by other researchers (Constatin *et al* 2004; Martinez *et al* 2004).

The electrical resistivity of CrN thin films at different temperatures were plotted against different N_2 flow rates and are shown in figure 5b. The electrical resistivity of pure Cr thin film (0 sccm) is $1{\cdot}7 \times 10^{-4}$ Ω cm and it increases heavily, increasing the sccm of N_2 up to 15. Beyond that, resistivity of the films exponentially decreases. The increasing trend of the electrical resistivity is due to the increase of impurity defect: for low concentrations of the N atoms occupy the interstitial position into the Cr structure. It may also be attributed to a decrease of the carrier density due to the nitrization of Cr (Ando and Suzuki 1997). By further increasing the nitrogen flow rate up to 20 sccm, the lattice configuration of CrN becomes progressively dominant, and some excessive N atom could insert into CrN lattice, as shown in the shift of the X-ray diffraction lines in figure 1. with the consequent decrease of resistivity. The over stoichiometric of nitrogen atoms doped in CrN lattices will act as an impurity, thereby inducing a decrease of electrical resistivity (Inoue *et al* 2002; Zhang *et al* 2007).

4. Conclusions

The chromium nitride thin films were successfully deposited on glass substrates and Si (100) wafers at different nitrogen flow rates by d.c. magnetron sputtering. XRD analysis indicated that wide range of phases Cr, Cr_2N, and CrN could be formed by varying the N_2 content in the deposition process. The grain size increases with the increase in the nitrogen flow rate. SEM image showed columnar and denser microstructure with varying nitrogen flow rate. The CrN films deposited at low nitrogen flow rate showed that the electrical resistivity correspond to a metallic-like behaviour and the films prepared at N_2 flow rate of 15 sccm and above showed a semiconducting behaviour.

Acknowledgements

One of the authors (BS) thanks the Department of Atomic Energy (DAE), Board of Research in Nuclear Sciences (BRNS), Mumbai, for a research grant (Sanction No 2006/37/37/BRNS/2068) and the Japan Society for the Promotion of Science, Japan, for the award of a FY 2011 JSPS Long term Invitation fellowship.

References

Albano C, Jeff Th and De Hosson M 2006 *Nanostructured coatings* (New York: Springer) p.183

Ando E and Suzuki S 1997 *J. Non-Cryst. Solids* **218** 68

Barshilia H C, Selvakumar N, Deepthi B and Rajam K S 2006 *Surf. Coat. Technol.* **201** 2193

Chen H Y, Han S and Shih H C 2004 *Mater. Lett.* **58** 2924

Conde A, Nivas C, Crisobal A B and de Damborenea J 2006 *Surf. Coat. Technol.* **201** 2690

Constatin C, Haider M B, Ingram D and Smith A R 2004 *Appl. Phys. Lett.* **85** 6371

Cunha L, Andritschky M, Pischow K and Wang Z 1999 *Thin Solid Films* **355–356** 466

Deniel R, Mahrtinschitz K J, Keckes J and Mitterer 2009 *J. Phys. D: Appl. Phys.* **42** 1

Fuentes G G *et al* 2005 *J. Mater. Process. Technol.* **167** 415

Gao X D *et al* 2007 *Phys. Status Solidi (a)* **204** 1130

Grips W, Ezhilselvi V, Barshilia H C and Rajam K S 2006 *Electrochim. Acta* **51** 346

Huang P K and Yeh J W 2009 *Surf. Coat. Technol.* **203** 1891

Huang J H, Ho C H and Yu G P 2007 *Mater. Chem. Phys.* **102** 31

Inoue S, Okada F and Koterazawa K 2002 *Vacuum* **66** 227

Inoue S, Okada F and Koterazawa K 2009 *Vacuum* **66** 231

Li R L, Tu J P, Hong C F, Liu D G and Sun H L 2009 *Surf. Coat. Technol.* **204** 470

Lin J, Wu Z L, Zhang X H, Mishra B, Moore J J and Sproul W D 2009 *Thin Solid Films* **517** 1887

Martinez E, Sanjines R, Banakh O and Levy F 2004 *Thin Solid Films* **447–448** 332

Novakovic M, Popovic M, Perusko D, Radovic I, Milinovic V and Milosavljevic M 2007 *Mater. Sci. Forum* **555** 35

Novinrooz A J and Seyedi H 2006 *J. Achieve. Mater. Manufacturing. Eng.* **17** 189

Olaya J J, Rodil S E, Muhl S and Sanchez E 2005 *Thin Solid Films* **474** 119

Olaya J J, Wei G, Rodil S E, Muhl S and Bushan B 2007 *Vacuum* **81** 610

Pelleg J, Zevin L Z, Lungo S and Croitoru N 1991 *Thin Solid Films* **197** 117

Ramos H J and Valmoria N B 2004 *Vacuum* **73** 549

Shen L, Xu S, Sun N, Cheng T and Cui Q 2008 *Mater. Lett.* **62** 1469

Shukla G and Khare A 2008 *Appl. Suf. Sci.* **255** 2057

Wei G, Rar A and Barnard J A 2001 *Thin Solid Films* **398–399** 460

Yoo Y H, Hong J H, Kim J G, Lee H Y and Han J G 2007 *Surf. Coat. Technol.* **201** 9518

Zhang G A, Yan P X, Wang P, Chen Y M and Zhang J Y 2007 *Mater. Sci. Engg.* **A460–461** 301

Zhao Z B, Rek Z U, Yalisove S M and Bilello J C 2004 *Surf. Coat. Technol.* **185** 329

Zou C W, Wang H J, Li M, Liu C S, Gou L P and Fu D J 2009 *Vacuum* **83** 1086